Two-Stage Optimum Design Method For Surface Acoustic Wave Duplexers Using Differential Evolution Algorithms

Kiyoharu Tagawa

***Abstract*—This paper proposes a novel computer-aided design method to decide on optimal structures of Surface Acoustic Wave (SAW) duplexers, which are used widely in the radio circuits of mobile communication systems. By using the proposed design method, engineers' knowledge can be easily reflected in the structure of SAW duplexer. The proposed design method is based on the computer simulation of SAW duplexer and composed of two stages: exploration and exploitation. In the first or exploration stage, the structural design of a target SAW duplexer is formulated as a constraint satisfaction problem. Then, by using an extended version of a recently-developed evolutionary algorithm, namely Differential Evolution (DE), various feasible solutions are obtained for the constraint satisfaction problem. In the second or exploitation stage, for deciding on an optimal structure of the SAW duplexer by considering the feasible solutions obtained in the first stage and the knowledge of engineers, the structural design of the SAW duplexer is reformulated again as a constrained optimization problem. Besides, for solving the constrained optimization problem effectively, another version of DE is contrived. The usefulness of the two-stage design method is also demonstrated through the structural design of a practical SAW duplexer that consists of four SAW resonators and two SAW filters.

***Keywords*—Computer-aided design, constrained optimization, evolutionary computation, optimum design, SAW duplexer.

I. Introduction

SURFACE Acoustic Wave (SAW) is an acoustic wave traveling along the surface of a material exhibiting elasticity. SAW devices are mechanical and electrical devices that use the acoustic wave in electronic components to provide a number of different functions including delay lines, resonators, filters, and so on [1]–[4]. Recently, SAW duplexers are used widely in the radio circuits of mobile communication systems such as cellular phones, smart phones, and Personal Digital Assistants (PADs). Incidentally, the duplexer is a key device for the radio circuits of various communication systems that isolates a receiver (Rx) from a transmitter (Tx) while permitting them to share a common antenna (ANT). Furthermore, SAW duplexers can provide small, thin, rugged, and cost competitive duplexers with outstanding frequency response characteristics [5]–[8].

SAW devices have one or more specific electrodes, which are called Inter-Digital Transducers (IDTs), to convert acoustic waves to electrical signals and vice versa by exploiting the piezoelectric effect of certain materials. Besides, SAW devices have several reflectors to restrain the spread of acoustic waves. Therefore, the frequency response characteristics of a SAW device is governed primarily by its geometrical structure, namely the configurations of IDTs and reflectors fabricated on a piezoelectric substrate. By deciding on an appropriate structure of the SAW device, we can carry out a desirable function.

In order to avoid the repetition of the design by trial and error, the structural design of a SAW device is often formulated as an optimization problem. After that, for solving the optimization problem, the optimum design method that combines an optimization algorithm with the simulator of the SAW device is used [9]–[14]. Author has also reported such an optimum design method for Double Mode SAW (DMS) filters by using a recently-developed evolutionary algorithm, namely Differential Evolution (DE) [14]. Incidentally, DE is arguably one of the most powerful optimization algorithms in current use. Because of its simple but powerful searching capability, DE has been used in several scientific and engineering applications [15]–[18]. The conventional optimum design method of DMS filters could reduce the cost and time spent for their developments. However, unlike DMS filters, not only the structure but also the function of the SAW duplexer is so complex. Therefore, we can't easily formulate the structural design of the SAW duplexer as an optimization problem. In other words, it is very hard to define directly the objective function and the design space for predicting and improving the quality of the SAW duplexer in terms of performance, robustness, and yield.

In this paper, a novel computer-aided design method of SAW duplexers is proposed. The proposed design method consists of two stages, namely exploration and exploitation. By using the proposed two-stage design method, engineers' knowledge can be easily reflected in the structure of SAW duplexer. As stated above, SAW duplexers usually have complex structures. For example, SAW duplexer to be designed in this paper consists of two DMS filters and four SAW resonators fabricated on a piezoelectric substrate. Therefore, in the structural design of the SAW duplexer, a number of design parameters have to be considered. Furthermore, the SAW duplexer must be designed for operation in frequency bands used by Rx and Tx, and must provide the frequency separation between Rx and Tx. In the first or exploration stage, the structural design of a SAW duplexer is

K. Tagawa is with the School of Science and Engineering, Kinki University, 3-4-1 Kowakae, Higashi-Osaka, 577-8502 Japan (phone: +81-6-6721-2332; fax: +81-6-6727-2024; e-mail: tagawa@info.kindai.ac.jp).

formulated as a constraint satisfaction problem instead of an optimization problem. The solutions that satisfy all constraints of the problem are called feasible ones. For the constraint satisfaction problem, we need to find as many feasible solutions as possible. In order to obtain various feasible solutions at one time, we propose a new DE-based algorithm called DE for Constraint Satisfaction (DECS). DECS has an archive to store all feasible solutions found so far. Through the analysis of the feasible solutions obtained by DECS, we can estimate the feasible region in the design space of the SAW duplexer.

In the second or exploitation stage, for choosing the most desirable solution within the feasible region estimated in the first stage, the structural design of the above SAW duplexer is reformulated again as a constrained optimization problem. In addition to the information about the SAW duplexer obtained in the first stage, the knowledge, wisdom, and preference of engineers can be used to define the constrained optimization problem. For solving the constrained optimization problem effectively, another DE-based algorithm, which is called DE for Constrained Optimization (DECO), is also proposed.

The rest of this paper is organized as follows. Section II explains the structure of SAW duplexer. Besides, the network model of SAW duplexer is derived. Section III formulates the structural design of SAW duplexer as a constraint satisfaction problem. In order to obtain various feasible solutions for the constraint satisfaction problem, a new DE-based algorithm, or DECS, is proposed in Section IV. Section V summarizes the first stage of the proposed two-stage design method. Section VI provides the second stage of the two-stage design method. In the second stage, considering the outcome of the first stage in addition to engineers' knowledge, the structural design of SAW duplexer is reformulated again as a constrained optimization problem. Furthermore, another DE-based algorithm, or DECO, is proposed to solve the constrained optimization problem. Through the structural design of a practical SAW duplexer, the usefulness of the two-stage design method is also demonstrated in Section VI. Finally, Section VII concludes the paper.

II. SAW DUPLEXER

A. Structure of SAW Duplexer

Fig. 1 illustrates two elemental components of various SAW devices, namely Inter-Digital Transducers (IDT) and Short Metal Strip Array (SMSA). IDT shown in Fig. 1(a) is assembled from two comb-shaped facing electrodes, which are referred to as fingers and used to excite and detect acoustic waves. On the other hand, SMSA shown in Fig. 1(b) is assembled from a number of metal strips and used to reflect acoustic waves.

Fig. 2 shows the basic structure of SAW duplexer that consists of four SAW resonators and two DMS filters. Each of SAW resonators consists of three elemental components: one IDT sandwiched between two SMSAs. On the other hand, each of DMS filters consists of five elemental components: three IDTs sandwiched between two SMSAs. All the parts of the SAW duplexer in Fig 2, namely four SAW resonators and two DMS filters, are fabricated on a piezoelectric substrate.

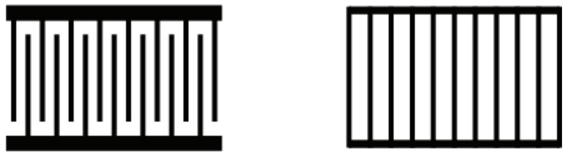

(a) IDT (b) SMSA

Fig. 1 Elemental components of SAW devices

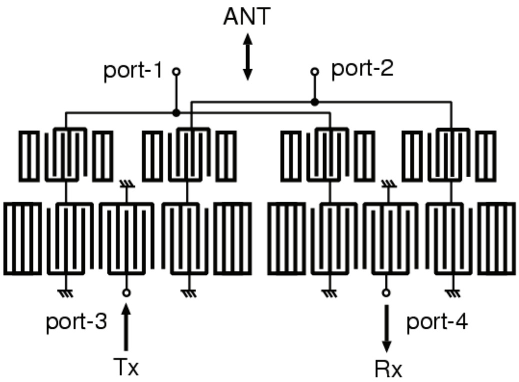

Fig. 2 Structure of SAW duplexer

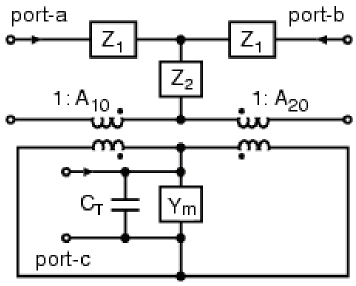

Fig.3 Equivalent circuit model of IDT

A pair of port-1 and port-2 of the SAW duplexer in Fig. 2 is connected to a common ANT and works as a balanced port for operating a differential mode signal [19]. On the other hand, port-3 and port-4 are connected to Tx and Rx, respectively, and work as normal ports for operating single mode signals. The two DMS filters connected to port-3 and port-4 are band-pass filters that provide two separate pass-bands for Tx and Rx.

B. Network Model of SAW Duplexer

In order to evaluate the frequency response characteristics of SAW duplexer through the computer simulation, we derive a network model of SAW duplexer. First of all, the behavior of IDT can be analyzed by using a three-port equivalent circuit model shown in Fig. 3: port-a and port-b are acoustic ports, while port-c is an electric port. In the equivalent circuit model of IDT, the values of impedances Z_1 and Z_2, admittance Y_m, and capacitance C_T depend on the shape of IDT such as the number and the length of fingers [20]. Besides, a two-port equivalent circuit model of SMSA can be also derived by shorting the electric port (port-c) of the equivalent circuit model of IDT.

The SAW duplexer shown in Fig. 2 is composed of a lot of elemental components, namely IDTs and SMSAs. Because all the elemental components of the SAW duplexer are connected acoustically in cascade on a piezoelectric substrate, a whole circuit model of the SAW duplexer can be made up from the equivalent circuit models of its elemental components in the same way with DMS filters [14]. Furthermore, by terminating the respective ports with characteristic impedances, we can transform the whole circuit model of the SAW duplexer into the network model represented by a scattering matrix S as

$$\begin{bmatrix} b_1 \\ b_2 \\ b_3 \\ b_4 \end{bmatrix} = S \begin{bmatrix} a_1 \\ a_2 \\ a_3 \\ a_4 \end{bmatrix} = \begin{bmatrix} s_{11} & s_{12} & s_{13} & s_{14} \\ s_{21} & s_{22} & s_{23} & s_{24} \\ s_{31} & s_{32} & s_{33} & s_{34} \\ s_{41} & s_{42} & s_{43} & s_{44} \end{bmatrix} \begin{bmatrix} a_1 \\ a_2 \\ a_3 \\ a_4 \end{bmatrix} \tag{1}$$

where a_n and b_n (n=1, 2, 3, 4) denote the input- and output-signals of the port-n of the SAW duplexer in Fig. 2. Besides, each s-parameter s_{nm} in the scattering matrix S provides the transmission characteristic from port-n to port-m.

As stated above, a pair of port-1 and port-2 of the SAW duplexer works as a balanced port. In order to evaluate the frequency response characteristics of the SAW duplexer strictly, differential mode signals need to be segregated from common mode signals at the balanced port. Therefore, according to the balanced network theory [21], the input- and output-signals a_n and b_n (n=1, 2) of the balanced port are converted into the input- and output-signals a_d and b_d of differential mode as

$$\left[\begin{aligned} a_d &= \frac{1}{\sqrt{2}}(a_1 - a_2), \\ b_d &= \frac{1}{\sqrt{2}}(b_1 - b_2). \end{aligned} \right. \tag{2}$$

Similarly, the input- and output-signals a_n and b_n (n=1, 2) of the balanced port of the SAW duplexer are also converted into the input- and output-signals a_c and b_c of common mode as

$$\left[\begin{aligned} a_c &= \frac{1}{\sqrt{2}}(a_1 + a_2), \\ b_c &= \frac{1}{\sqrt{2}}(b_1 + b_2). \end{aligned} \right. \tag{3}$$

From (2) and (3), the network model in (1) is transformed into another form with the mix-mode s-parameters as

$$\begin{bmatrix} b_d \\ b_c \\ b_3 \\ b_4 \end{bmatrix} = TST^{-1} \begin{bmatrix} a_d \\ a_c \\ a_3 \\ a_4 \end{bmatrix} = \begin{bmatrix} s_{dd} & s_{dc} & s_{d3} & s_{d4} \\ s_{cd} & s_{cc} & s_{c3} & s_{c4} \\ s_{3d} & s_{3c} & s_{33} & s_{34} \\ s_{4d} & s_{4c} & s_{43} & s_{44} \end{bmatrix} \begin{bmatrix} a_d \\ a_c \\ a_3 \\ a_4 \end{bmatrix}, \tag{4}$$

where the matrix T is described as

$$T = \frac{1}{\sqrt{2}} \begin{bmatrix} 1 & 1 & 0 & 0 \\ -1 & 1 & 0 & 0 \\ 0 & 0 & \sqrt{2} & 0 \\ 0 & 0 & 0 & \sqrt{2} \end{bmatrix}. \tag{5}$$

III. Constraint Satisfaction Problem

Desirable frequency response characteristics of the SAW duplexer can be specified by a set of constraints for them. Thus the structural design of the SAW duplexer is formulated as a constraint satisfaction problem. In order to describe the shapes of the elemental components of the SAW duplexer, we choose D design parameters $\vec{x} = (x_1, \cdots, x_j, \cdots, x_D)$ including the length and the number of IDT's fingers. The design parameters' values are limited by the lower $\underline{x}_j$ and the upper $\overline{x}_j$ bounds as

$$\underline{x}_j \le x_j \le \overline{x}_j, \quad j = 1, \cdots, D. \tag{6}$$

From the network model in (4), we define three performance criteria to evaluate the frequency response characteristics of the SAW duplexer, which depend on the above design parameter $\vec{x}$ and vary with the frequency. Let $\omega \in \Omega$ be a frequency point sampled from the frequency bands Ω used by Tx and Rx.

Firstly, from the mix-mode s-parameter s_{d3} of a_3 to b_d in (4), the transmission characteristic of Tx to ANT is defined as

$$\Gamma_T(\vec{x}, \omega) = 20 \log_{10}(|s_{d3}(\vec{x}, \omega)|). \tag{7}$$

Secondly, from the mix-mode s-parameter s_{4d} of a_d to b_4, the transmission characteristic of ANT to Rx is defined as

$$\Gamma_R(\vec{x}, \omega) = 20 \log_{10}(|s_{4d}(\vec{x}, \omega)|). \tag{8}$$

Finally, from the mix-mode s-parameter s_{43} of a_3 to b_4, the transmission characteristic of Tx to Rx is defined as

$$\Gamma_I(\vec{x}, \omega) = 20 \log_{10}(|s_{43}(\vec{x}, \omega)|). \tag{9}$$

Now, we define some constraints for the above performance criteria. Firstly, let Ω_1 be a set of frequency points $\omega \in \Omega_1$ sampled from the pass-band of Tx. Besides, let Ω_2 be a set of frequency points sampled from the stop-band of Tx. Thereby, two constraints for the performance criterion defined in (7) are given by its lower $L_T(\omega)$ and upper $U_T(\omega)$ bounds as

$$\left[\begin{aligned} g_1(\vec{x}, \omega) &= L_T(\omega) - \Gamma_T(\vec{x}, \omega) \le 0, \quad \omega \in \Omega_1, \\ g_2(\vec{x}, \omega) &= \Gamma_T(\vec{x}, \omega) - U_T(\omega) \le 0, \quad \omega \in \Omega_2. \end{aligned} \right. \tag{10}$$

Secondly, let Ω_3 and Ω_4 be the sets of frequency points sampled, respectively, from the pass- and stop-bands of Rx. Thereby, two constraints for the performance criterion in (8) are given by its lower $L_R(\omega)$ and upper $U_R(\omega)$ bounds as

$$\begin{cases} g_3(\vec{x},\omega) = L_R(\omega) - \Gamma_R(\vec{x},\omega) \le 0, & \omega \in \Omega_3, \\ g_4(\vec{x},\omega) = \Gamma_R(\vec{x},\omega) - U_R(\omega) \le 0, & \omega \in \Omega_4. \end{cases} \tag{11}$$

Finally, let Ω_5 be a set of frequency points sampled from both bands of Tx and Rx. Then a constraint for the performance criterion in (9) is given by its upper $U_I(\omega)$ bound as

$$g_5(\vec{x},\omega) = \Gamma_I(\vec{x},\omega) - U_I(\omega) < 0, \quad \omega \in \Omega_5. \tag{12}$$

Let X be a set of the design parameters $\vec{x} = (x_1, \cdots, x_D)$ that satisfy the boundary constraints in (6). From now on, the set X is referred to as the design space of the SAW duplexer. For the constraint satisfaction problem, we look for a number of solutions $\vec{x} \in X$ that satisfy all inequality constraints in (10), (11), and (12). As stated above, the solutions $\vec{x} \in X$ that satisfy all constraints are called feasible solutions. Even though the existence of feasible solution is not guaranteed theoretically, a number of feasible solutions usually exist for the constraint satisfaction problem. Therefore, we define the feasible region F ($F \subseteq X$) as a whole set of feasible solutions $\vec{x} \in F \subseteq X$.

IV. Algorithm for Constraint Satisfaction

A. Representation

In order to obtain a number of feasible solutions $\vec{x} \in F \subseteq X$ for the constraint satisfaction problem at one time, we employ a new DE-based algorithm called DECS [22]. A purpose of the first stage of the design method is to estimate the feasible region $F \subseteq X$ from the set of feasible solutions obtained by DECS. Like the canonical DE [15], DECS has N_P tentative solutions, which are referred to as individuals, in the population P. The i-th individual $\vec{x}_i \in P$ ($i = 1, \cdots, N_P$) of the population P is represented by a D-dimensional real vector as

$$\vec{x}_i = (x_{1,i}, \cdots, x_{j,i}, \cdots, x_{D,i}) , \tag{13}$$

where $x_{j,i} \in R$ and $\underline{x}_j \le x_{j,i} \le \overline{x}_j, \quad j = 1, \cdots, D.$

Let $rand[0, 1]$ be the random number generator that returns a uniformly distributed random number in the range [0, 1]. Thereby, the initial population is generated randomly as

$$x_{j,i} = rand[0,1](\overline{x}_j - \underline{x}_j) + \underline{x}_j , \tag{14}$$

where $j = 1, \cdots, D$ and $i = 1, \cdots, N_P$.

B. DE Strategy

DECS uses the strategy of DE to generate a new individual. Even though various strategies have been proposed for DE [16], we employ a basic strategy named "DE/rand/1/bin" [15]. In the basic strategy, each of the individual $\vec{x}_i \in P$ $(i = 1, \cdots, N_P)$ is assigned to "the target vector" in turn. Except for the target vector, three mutually different individuals, say $\vec{x}_{i1}$, $\vec{x}_{i2}$, and $\vec{x}_{i3}$ $(i \ne i1 \ne i2 \ne i3)$, are selected randomly from P. After that, a new individual $\vec{u} = (u_1, \cdots, u_j, \cdots, u_D) \in R^D$ called "the trial vector" is generated from the four individuals as

$$u_j = \begin{cases} x_{j,i1} + S_F\ (x_{j,i2} - x_{j,i3}), & \text{if } rand[0,1] \le C_R, \\ x_{j,i}, & \text{otherwise,} \end{cases} \tag{15}$$

where the scale factor $S_F \in R, (0 < S_F < 2)$ and the crossover rate $C_R \in [0,1]$ are control parameters given by the user.

If the strategy in (15) makes an element u_j of the trial vector $\vec{u}$ outside the range [0, 1], it is returned to the range as

$$u_j = \begin{cases} x_{j,i1} + rand[0,1](\underline{x}_j - x_{j,i1}), & \text{if } u_j < \underline{x}_j, \\ x_{j,i1} + rand[0,1](\overline{x}_j - x_{j,i1}), & \text{if } u_j > \overline{x}_j. \end{cases} \tag{16}$$

A design parameter x_j $(j = 1, \cdots, D)$ in (6) takes either a continuous value $x_j \in R$ or a discrete value $x_j \in Q$ spaced apart by an interval $e_j \in R$, where Q is the set of discrete design parameters. However, every element $x_{j,i} \in R$ of the individual $\vec{x}_i \in P$ takes a real value. Therefore, elements $x_{j,i} \in R$ of the individual $\vec{x}_i \in P$ corresponding to discrete design parameters $x_j \in Q$ are converted, respectively, into $x_j \in Q$ as

$$x_j = round\left(\frac{x_{j,i}}{e_j}\right) e_j \tag{17}$$

where $round(r)$ rounds a real $r \in R$ to the nearest integer.

Now, we have to measure the goodness of the individual $\vec{x}_i \in P$ that corresponds to a solution $\vec{x} \in X$. Therefore, from the five constraints shown in (10), (11), and (12), we define the penalty function $g(\vec{x}_i)$ for $\vec{x}_i \in P$ to be minimized as

$$g(\vec{x}_i) = \sum_{p=1}^{5} \sum_{\omega \in \Omega_p} \max\left\{ g_p(\vec{x}_i, \omega), 0 \right\} \tag{18}$$

where $g(\vec{x}_i) = 0$ holds for a feasible solution $\vec{x} \in F$, while $g(\vec{x}_i) > 0$ holds for an infeasible solution $\vec{x} \notin F$.

C. DECS Algorithm

DECS is an extended version of Dispersive DE (DDE) proposed by authors [23]. Therefore, DECS is based on the steady-state model that uses only one population *P*. First of all, the initial population *P* is generated randomly as shown in (4). DECS generates more than one trial vector $\vec{u}$ from each target vector $\vec{x}_i \in P$. If one of the newborn trial vectors $\vec{u}$ is not worse than the target vector $\vec{x}_i \in P$, the target vector $\vec{x}_i \in P$ is replaced by the new excellent trial vector $\vec{u}$ immediately. In order to obtain a number of feasible solutions, DECS has an archive *A* to store all feasible solutions found so far. If a newborn trial vector $\vec{u}$ corresponds to a feasible solution $\vec{x} \in F$, it is added to the archive *A*. The control parameters of DECS are the maximum number of the penalty function evaluation N_E, the population size N_P, the maximum number of the trial vectors generated from one target vector N_T, and two control parameters S_F and C_R used by the basic strategy in (15). Thereby, the DECS algorithm works as follows:

[DECS Algorithm]

1) Initialize the archive such as $A = \phi$.
2) Randomly generate $\vec{x}_i \in P\ (i = 1, \cdots, N_P)$.
3) For all $\vec{x}_i \in P$, evaluate $g(\vec{x}_i)$. Let $k=N_P$.
4) If $k>N_E$ holds then output all feasible solutions $\vec{x}_i \in A$.
5) For each $\vec{x}_i \in P$, repeat N_T times from Steps 6 to 10.
6) Randomly select $\vec{x}_{i1}$, $\vec{x}_{i2}$, and $\vec{x}_{i3}$ from *P*.
7) Generate a trial vector $\vec{u}$ by (15) and (16).
8) Evaluate $g(\vec{u})$. Let $k=k+1$.
9) If $g(\vec{u}) \le g(\vec{x}_i)$ holds then replace $\vec{x}_i \in P$ by $\vec{u}$ such as $\vec{x}_i = \vec{u}$ and $g(\vec{x}_i) = g(\vec{u})$.
10) If $g(\vec{u}) = 0$ holds then $A = A \cup \{\vec{u}\}$.
11) Return to Step 4.

V. First Stage of Design Method

A. Setup of Computational Experiment

The simulator of the SAW duplexer based on the network model in (4) was made by MATLAB and converted into the library used by the Java language. The specifications for the SAW duplexer, namely the upper and lower bounds of the performance criteria, were specified at 301 frequency points $\omega \in \Omega$ within the range: 700～1000[MHz]. In order to describe the structure of the SAW duplexer, we selected *D*=18 design parameters with their upper and lower bounds. The design space of the SAW duplexer was given exactly by Table I.

The proposed DECS was coded by Java and executed on a commodity computer (CPU: Intel Core i7; 3.33[GHz]; OS: Windows XP). The above library of the SAW duplexer's simulator was included in the program of DECS. From a prior outcome of an experiment, the control parameters of DECS were chosen as N_E=10000, N_P=100, N_T=5, S_F=0.5, and C_R=0.9. Thereby, in order to a set of obtain feasible solutions, DECS was applied to the constraint satisfaction problem.

Table I Design space of SAW duplexer

x_j	$[\underline{x}_j,\ \overline{x}_j]$	x_j	$[\underline{x}_j,\ \overline{x}_j]$
x_1	[250, 350]	x_{10}	[45, 65]
x_2	[3900, 4030]	x_{11}	[2.20, 2.40]
x_3	[16.5, 24.5]	x_{12}	[16.5, 24.5]
x_4	[12, 20]	x_{13}	[12, 20]
x_5	[35, 65]	x_{14}	[45, 65]
x_6	[2.26, 2.46]	x_{15}	[2.22, 2.32]
x_7	[250, 350]	x_{16}	[55, 95]
x_8	[3900, 4030]	x_{17}	[35, 65]
x_9	[55, 95]	x_{18}	[2.00, 2.20]

x_1 : length of electrodes in all filters [um]
x_2 : thickness of electrodes in all filters [A]
x_3 : number of center IDT's fingers in Tx filter
x_4 : number of side IDT's fingers in Tx filter
x_5 : number of SMSA's strips in Tx filter
x_6 : finger pitch of IDT in Tx filter [um]
x_7 : length of electrodes in all resonators [um]
x_8 : thickness of electrodes in all resonators [A]
x_9 : number of IDT's fingers in Tx resonators
x_{10} : number of SMSA's strips in Tx resonators
x_{11} : finger pitch of IDT in Tx resonators [um]
x_{12} : number of center IDT's fingers in Rx filter
x_{13} : number of side IDT's fingers in Rx filter
x_{14} : number of SMSA's strips in Rx filter
x_{15} : finger pitch of IDT in Rx filter [um]
x_{16} : number of IDT' fingers in Rx resonators
x_{17} : number of SMSA's strips in Rx resonators
x_{18} : finger pitch of IDT in Rx resonators [um]

B. Result of Computational Experiment

By only one trial of DECS, we could obtain $|A|$=5453 feasible solutions $\vec{x} \in A$ of the constraint satisfaction problem. Fig. 4 shows the range of the design parameters $x_j\ (j = 1, \cdots, D)$ included in the feasible solutions $\vec{x} \in A \subseteq F$, where the respective design parameters' values are normalized between 0 and 1. The maximum and minimum values of the design parameters $x_j\ (j = 1, \cdots, D)$ included in $\vec{x} \in A \subseteq F$ are plotted by broken lines in Fig. 4. The center values of those design parameters are also plotted by a solid line. From Fig. 4, we get a rough image of the feasible region $F \subseteq X$. For example, the available value of a sensitive design parameter is restricted within a narrow interval. Besides, several design parameters have no influence upon the performance of the SAW duplexer.

The frequency response characteristics of the SAW duplexer achieved by one of the feasible solutions $\vec{x} \in A$ are shown in Figs. 5 and 6. Fig. 5 shows the band-pass characteristics of Tx to ANT and ANT to Rx. The upper and lower bounds for them are described by broken lines in Fig. 5 too. Fig. 6 shows the transmission characteristics of Tx to Rx, which is the isolation characteristic between Tx and Rx. The upper bound of the isolation characteristic is also shown by broken line in Fig. 6.

From Figs. 5 and 6, we can confirm that the feasible solution $\vec{x} \in A$ satisfies all constraints shown in (10), (11), and (12).

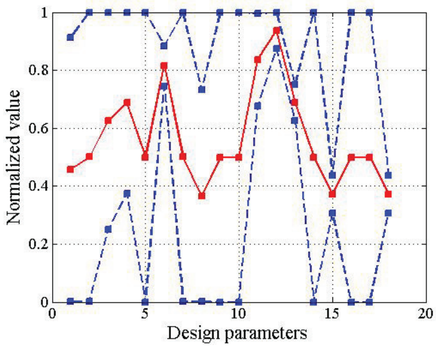

Fig. 4 Design parameters of feasible solutions

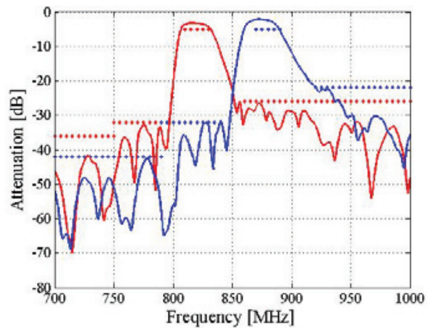

Fig. 5 Band-pass characteristics by a feasible solution

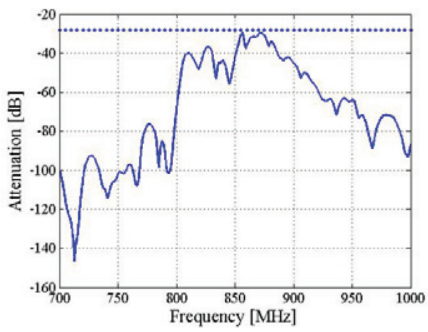

Fig. 6 Isolation characteristic by a feasible solution

Under the assumption that the feasible region F consists of only one island that is simply connected and convex, a solution $\vec{z} = (z_1, \cdots, z_j, \cdots, z_D)$ composed by the center values z_j of the respective design parameters x_j in Fig. 4 exists at the center of the feasible region F. The literature [24] asserts that such a solution $\vec{z}$ is also feasible and gives a robust solution of the design problem against the influence of uncertain factors.

The frequency response characteristics of the SAW duplexer achieved by the center solution $\vec{z}$ are shown in Figs. 7 and 8. Fig. 7 shows the band-pass characteristics of Tx to ANT and ANT to Rx with their upper and lower bounds. Fig. 8 shows the isolation characteristics with its upper bound. In Figs. 7 and 8, several upper and lower bounds have been violated. Thus the center solution $\vec{z} \in X$ in Fig. 4 is infeasible. Consequently, the feasible region $F \subseteq X$ may not be convex. Otherwise, there is an interaction between several design parameters.

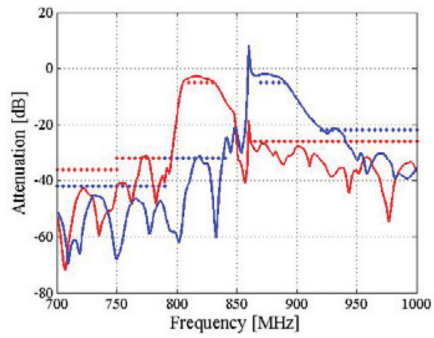

Fig. 7 Band-pass characteristics by the center solution

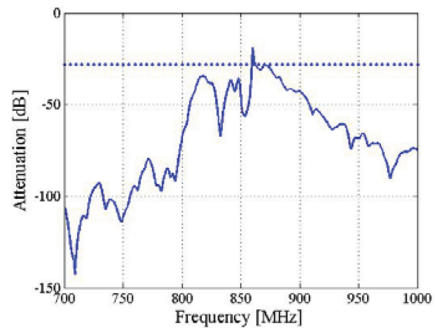

Fig. 8 Isolation characteristics by the center solution

VI. Second Stage of Design Method

A. Constrained Optimization Problem

In order to decide on an optimum structure of the SAW duplexer considering the result of the first stage, the structural design of the SAW duplexer is reformulated as a constrained optimization problem. First of all, by considering the feasible region $F \subseteq X$ which can be estimated from Fig. 4, we reduce the SAW duplexer's design space given by Table I. Exactly, we narrow the search range $[\underline{x}_j, \overline{x}_j]$ of several design parameters in Table I. Furthermore, we fix the values of several design parameters. As a result, we have only to decide on $\tilde{D}\ (\tilde{D} < D)$ design parameters $\vec{x} = (x_1, \cdots, x_{\tilde{D}})$ in the reduced design space of the SAW duplexer $\tilde{X} \subseteq X$. The isolation characteristic of the SAW duplexer in (9) is chosen for the objective function to be minimized. Consequently, from (9), (10), (11), and (12), the constrained optimization problem is formulated as

$$\begin{cases} \text{minimize} & f(\vec{x}) = \sum_{\omega \in \Omega_5} \Gamma_I(\vec{x}, \omega), \\ \text{subject to} & g_p(\vec{x}, \omega) \le 0,\ \omega \in \Omega_p\ (p = 1, \cdots, 5), \\ & \text{and } \vec{x} \in \tilde{X}. \end{cases} \tag{19}$$

In the constrained optimization problem shown in (19), we suppose that $\widetilde{X} \cap F \neq \phi$ holds. Then we look for the best feasible solution $\vec{x} \in F$ of the constraint satisfaction problem that minimizes the isolation characteristic $\Gamma_I(\vec{x}, \omega)$ in (9). The isolation characteristic is used both as the objective function $f(\vec{x})$ and the constraint $g_5(\vec{x}, \omega) \leq 0$ in (19). This is because a high isolation characteristic between Tx and Rx is desired for the SAW duplexer used in the modern radio circuit [5].

B. Algorithm for Constrained Optimization

In the second stage of the proposed design method, we decide on the best structure of the SAW duplexer from the optimum solution of the constrained optimization problem shown in (19). In order to solve the constrained optimization problem, we propose another version of DE named DECO. The proposed DECO is similar to Generalized DE [25] contrived to solve constrained optimization problems. However, as well as DECS, DECO is an extended version of DDE [23]. Therefore, DECO is based on the steady-state model and generates more than one trial vector $\vec{u}$ from one target vector $\vec{x}_i \in P$. Furthermore, in the comparison of $\vec{u}$ and $\vec{x}_i \in P$, DECO adopts the following selection criteria originally proposed by Deb [26]:

- If both solutions are infeasible, the one with the smaller penalty function value is preferred.
- If one solution is feasible and the other one is infeasible, the feasible solution wins.
- If both solutions are feasible, the one with the smaller objective function value wins.

The control parameters of DECO are the same as those of DECS. The DECO algorithm works as follows:

[DECO Algorithm]

1) Randomly generate initial $\vec{x}_i \in P \; (i = 1, \cdots, N_P)$.
2) For all $\vec{x}_i \in P$, evaluate $g(\vec{x}_i)$ and $f(\vec{x}_i)$. Let $k=N_P$.
3) If $k>N_E$ holds then output the best feasible solution $\vec{x}_i \in P \cap F$ that has the minimum $f(\vec{x}_i)$ value.
4) For each $\vec{x}_i \in P$, repeat N_T times from Steps 5 to 8.
5) Randomly select $\vec{x}_{i1}$, $\vec{x}_{i2}$, and $\vec{x}_{i3}$ from P.
6) Generate a trial vector $\vec{u}$ by (15) and (16).
7) Evaluate $g(\vec{u})$ and $f(\vec{u})$. Let $k=k+1$.
8) If one of the following conditions holds, replace $\vec{x}_i \in P$ by $\vec{u}$ such as $\vec{x}_i = \vec{u}$, $g(\vec{v}_i) = g(\vec{u})$, and $f(\vec{x}_i) = f(\vec{u})$.

$$\begin{cases} 0 < g(\vec{u}) \leq g(\vec{x}_i), \\ (g(\vec{u}) = 0) \wedge (g(\vec{x}_i) > 0), \\ (g(\vec{u}) = g(\vec{x}_i) = 0) \wedge (f(\vec{u}) \leq f(\vec{x}_i)). \end{cases}$$

9) Return to Step 3.

C. Result of Computational Experiment

Considering the design parameters of the feasible solutions shown in Fig. 4, we reduced the SAW duplexer's design space given by Table I. First of all, we fixed the values of sensitive design parameters to constant values. Besides, in order to miniaturize the SAW duplexer's size, we also fixed the length of electrodes to the minimum value in the feasible region. As a result, we could reduce the number of design parameters to be optimized from D=18 to $\widetilde{D} = 11$. Furthermore, we narrowed the search range $[\underline{x}_j, \overline{x}_j]$ of several design parameters given by Table I. Then we defined the reduced design space of the SAW duplexer $\widetilde{X} \subseteq X$ as shown in Table II, in which design parameters fixed to constants are putted in parentheses.

Like the constraint satisfaction problem, the upper and lower bounds of the performance criteria were specified at 301 frequency points $\omega \in \Omega$ within the range: 700～1000[MHz]. The proposed DECO was also coded by Java and executed on the commodity computer. The control parameters of DECO were the same as those of DECS. Thereby, DECO was applied to the constrained optimization problem shown in (19).

The design parameters' values $x_j \; (j = 1, \cdots, D)$ of the optimum solution obtained by DECO are plotted by solid line in Fig. 9, where the respective values are normalized between 0 and 1. As shown in Table II, several design parameters in Fig. 9 have been fixed in advance. The maximum and minimum values of all design parameters $x_j \; (j = 1, \cdots, D)$ included in the feasible solutions $\vec{x} \in A \subseteq F$ are plotted again by broken lines in Fig. 9, where they have been already shown in Fig. 4.

Table II Reduced design space of SAW duplexer

x_j	$[\underline{x}_j, \overline{x}_j]$	x_j	$[\underline{x}_j, \overline{x}_j]$
(x_1)	260	x_{10}	[45, 65]
x_2	[3900, 4030]	x_{11}	[2.30, 2.40]
x_3	[18.5, 24.5]	(x_{12})	24.5
x_4	[15, 20]	(x_{13})	18
x_5	[35, 65]	x_{14}	[45, 65]
(x_6)	2.42	(x_{15})	2.26
(x_7)	260	x_{16}	[55, 95]
x_8	[3900, 4000]	x_{17}	[35, 65]
x_9	[55, 95]	(x_{18})	2.07

(x_1) : length of electrodes in all filters [um]
(x_6) : finger pitch of IDT in Tx filter [um]
(x_7) : length of electrodes in all resonators [um]
(x_{12}) : number of center IDT's fingers in Rx filter
(x_{13}) : number of side IDT's fingers in Rx filter
(x_{15}) : finger pitch of IDT in Rx filter [um]
(x_{18}) : finger pitch of IDT in Rx resonators [um]

The frequency response characteristics of the SAW duplexer achieved by the optimum solution are shown in Figs. 10 and 11. Fig. 10 shows the band-pass characteristics of Tx to ANT and ANT to Rx with their upper and lower bounds. Fig. 11 shows the isolation characteristics with its upper bound. From Figs. 10 and 11, we can confirm that the optimum solution is feasible. Furthermore, from the comparison of Fig. 6 and Fig. 11, the isolation characteristic in Fig. 11 is decreased obviously.

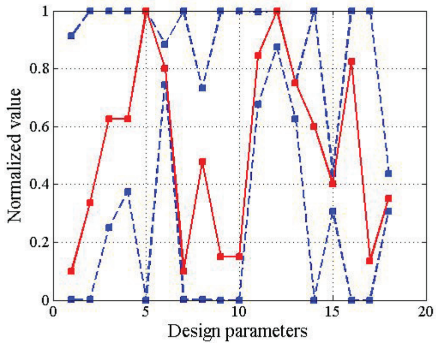

Fig. 9 Design parameters of the optimum solution

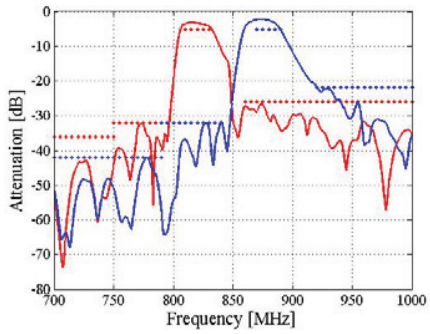

Fig. 10 Bans-pass characteristics by the optimum solution

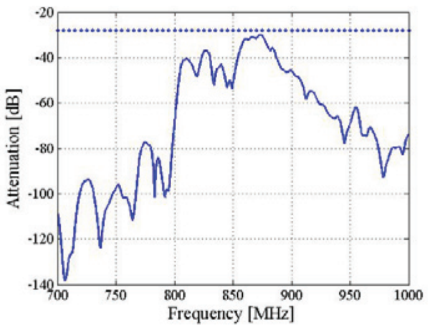

Fig. 11 Isolation characteristics by the optimum solution

VII. Conclusion

A computer-aided two-stage design method was proposed and applied to the structural design of a practical SAW duplexer. The SAW duplexer consisted of two DMS filters and four SAW resonators fabricated on a piezoelectric substrate. Dou to the complexity of its structure, it was difficult to formulate the structural design of the SAW duplexer as an optimization problem directly. Therefore, we contrived the two-stage design method for the structural design of the SAW duplexer. In the first stage of the proposed design method, the structural design of the SAW duplexer was formulated as a constraint satisfaction problem. Then, in order to obtain feasible solutions as many as possible, a new version of DE called DECS was applied to the constraint satisfaction problem. In the second stage of the proposed design method, considering the information about the SAW duplexer obtained in the first stage and the knowledge of engineers, the structural design of the above SAW duplexer is reformulated again as a constrained optimization problem. In order to an optimum solution of the constrained optimization problem effectively, namely an optimal structure of the SAW duplexer, another version of DE called DECO was applied to the constrained optimization problem. Finally, through the structural design of the practical SAW duplexer, the usefulness of the proposed two-stage design method was demonstrated.

The proposed two-stage design method can be applied to other SAW devices. Furthermore, the concept two-stage design method is applicable to various real-world applications.

Although the two-stage design method showed promising results, there are several issues which need to further research. If we can't find any feasible solution in the first stage, we have to loosen several constraints of the constraint satisfaction problem. Considering the result of the first stage, we may fix several design parameters to constants in the second stage. However, it doesn't make any guarantee that the constrained optimization problem has feasible solutions. If we can't find any feasible solution for the problem, we need to reconsider the design parameters to be fixed. In any case, the results of the proposed design method rely on the searching abilities of the optimization algorithms used in the first and second stages. Therefore, in our future works, we would like to improve DECS and DECO further by using the latest optimization techniques.

Acknowledgment

The research reported in this paper was supported in part by the Grant-in-Aid for Scientific Research (C) (No. 24560503) from Japan Society for the Promotion of Science (JSPS).

References

[1] K. Hashimoto, *Surface Acoustic Wave Devices in Telecommunications —Modeling and Simulation*, Springer, 2000.

[2] H. Meier, T. Baier, and G. Riha, "Miniaturization and advanced functionalities of SAW devices," *IEEE Trans. on Microwave Theory and Techniques*, vol. 49, no. 2, 2001, pp. 743–748.

[3] H. Nakamura, H. Nakanishi, T. Tsurunari, K. Matsunami, Y. Iwasaki, K. Hashimoto, and M. Yamaguchi, "Suppression of transverse mode spurious in SAW resonators on an $SiO_2/Al/LiNbO_3$ structure for wideband CDMA applications," *in Proc. IEEE Ultrasonics Symposium*, 2008, pp. 594–597.

[4] Y. S. Shmaliy, G. Cerda-Villafana, and O. Ibarra-Mamzano, "An analysis of errors in RFID SAW-tag systems with pulse position coding," *in Proc. 6th WSEAS Int. Conf. on Computer Engineering and Applications*, Harvard, Cambridge, USA, January, 2012, pp. 175–180.

[5] T. Shiba, M. Ooki, J. Hamasaki, O. Hikino, and Y. Fujita, "Study of high isolation and miniature SAW duplexer," *in Proc. IEEE Ultrasonics Symposium*, 2006, pp. 1060–1064.

[6] S. Inoue, J. Tsutsumi, T. Matsuda, M. Ueda, O. Ikata, and Y. Satoh, "Ultra-steep cut-off double mode SAW filter and its application to a PCS duplexer," *IEEE Trans. on Ultrasonics, Ferroelectrics, and Frequency Control*, vol. 54, no. 9, 2007, pp. 1882–1887.

[7] H. Nakamura, H. Nakanishi, T. Tsurunari, J. Fujiwara, Y. Hamaoka, and R. Goto, "Small-sized SAW duplexer on non-flat $SiO_2/Al/LiNbO_3$ structure for UMTS band I system," *in Proc. IEEE Ultrasonics Symposium*, 2010, pp. 1818–1821.

[8] T. Yamane, M. Mimura, D. Tamazaki, E. Fujimori, Y. Fujii, M. Yata, and H. Kando, "A miniaturized UMTS band II duplexer employing piezoelectric boundary acoustic wave," *in Proc. Asia-Pacific Microwave Conf.*, 2011, pp. 550–553.

[9] S. Goto and T. Kawakatsu, "Optimization of the SAW filter design by immune algorithm," *in Proc. IEEE Ultrasonics Ferroelectrics, and Frequency Control Joint 50th Anniversary Conf.*, 2004, pp. 600–603.
[10] A. Milewaki, E. Sedek, and S. Gawor, "Computer aided design of dispersive delay lines," *in Proc. 5th WSEAS Int. Conf. on Simulation, Modeling and Optimization*, Corfu, Greece, August, 2005, pp. 527–530.
[11] N. Khalil, A. Zaki, M. B. Saleh, and H. Ali, "Optimum design of MEMS-SAW filters for wireless system applications," *in Proc. 5th WSEAS Int. Conf. on Circuits, Systems, Electronics, Control & Signal Processing*, Dallas, USA, November, 2006, pp. 14–19.
[12] K. Tagawa, "Simulation modeling and optimization technique for balanced surface acoustic wave filters," *in Proc. 7th WSEAS Int. Conf. on Simulation, Modeling and Optimization*, Beijing, China, September, 2007, pp. 295–300.
[13] K. Tagawa and H. Kim, "A local search technique for large-scale optimum design problems of double mode SAW filters," *WSEAS Trans. on Circuits and System*, Issue 1, vol. 6, 2007, pp. 1–8.
[14] K. Tagawa, "Evolutionary computation techniques for the optimum design of balanced surface acoustic wave filters," *in Proc. IEEE Conf. on Evolutionary Computation*, Hong Kong, June, 2008, pp. 299–304.
[15] R. Storn and K. Price, "Differential evolution — a simple and efficient heuristic for global optimization over continuous space," *Journal of Global Optimization*, vol. 11, no. 4, 1997, pp. 341–359.
[16] K. V. Price, R. M. Storn, and J. A. Lampinen, *Differential Evolution — A Practical Approach to Global Optimization*, Springer, 2005.
[17] A. Qing, *Differential Evolution — Fundamentals and Applications in Electrical Engineering*, John Wiley & Sons (Asia), Singapore, 2009.
[18] S. Das and P. N. Suganthan, "Differential evolution: a survey of the state-of-art," *IEEE Trans. on Evolutionary Computation*, vol. 15, no. 1, 2011, pp. 4–31.
[19] S. T. Wang and M-H. Chung, "Simulation of balanced surface acoustic wave (SAW) devices incorporating a modified four-port Mason's equivalent circuit model," *in Proc. 10th WSEAS Int. Conf. on Circuits*, Vouliagmeni, Athens, Greece, July, 2006, pp. 148–153.
[20] T. Kojima and T. Suzuki, "Fundamental equations of electro-acoustic conversion for an inter-digital surface-acoustic-wave transducer by using force factors," *Japan Journal of Applied Physics Supplement*, vol. 31, Supplement 31-1, 1992, pp. 194–197.
[21] D. E. Bockelman and W. R. Eisenstadt, "Combined differential and common-mode scattering parameters: theory and simulation," *IEEE Trans. on Microwave Theory and Techniques*, vol. 43, no. 7, 1995, pp. 1530–1539.
[22] K. Tagawa, "Exploration of SAW duplexer design space by modified differential evolution," *in Proc. 14th WSEAS Int. Conf. on Mathematical and Computational Methods in Science and Engineering*, Sliema, Malta, September, 2012, pp. 79–84.
[23] K. Tagawa and H. Takada, "Comparative study of extended sequential differential evolutions," *in Proc. 9th WSEAS Int. Conf. on Applications of Computer Engineering*, Penang, Malaysia, March, 2010, pp. 52–57.
[24] R. Storn, "System design by constraint adaptation and differential evolution," *IEEE Trans. on Evolutionary Computation*, vol. 3, no. 1, 1999, pp. 22–34.
[25] S. Kukkonen and J. Lampinen, "Constrained real-parameter optimization with generalized differential evolution," *in Proc. IEEE Conf. on Evolutionary Computation*, Vancouver, July, 2006, pp. 911–918.
[26] K. Deb, "An efficient constraint handling method for genetic algorithms," *Computer Models in Applied Mechanics and Engineering*, vol. 186, Issues 52–57, Elsevier, 2000, pp. 311–338.

Kiyoharu Tagawa received his M.E. and Ph.D. degrees from Kobe University, Kobe Japan, in 1993 and 1997, respectively. From 2005 to 2007, he served as an Associate Professor of the Faculty of Engineering, Kobe University. He is currently a Professor of the School of Science and Engineering, Kinki University, Osaka Japan. His research interests include evolutionary computation, concurrent programming, multi-objective optimization, and optimum design of SAW devices.